Int J Clin Exp Med 2020;13(10):7393-7405
www.ijcem.com /ISSN:1940-5901/IJCEM0117117

*Original Article*

# miR-217 enhances pancreatic β cell functions in type 2 diabetic mice by targeting the KRAS gene

Anjun Tan[1], Tianrong Li[3], Libo Ruan[3], Jingjing Yang[3], Yuanyuan Luo[3], Xi'nan Wu[2], Ling Li[1]

*[1]Biomedical Engineering Research Center, [2]The School of Public Health, Kunming Medical University, Kunming, Yunnan Province, China; [3]Department of Geriatric Medicine, The First People's Hospital of Yunnan Province, Kunming, Yunnan Province, China*

Received June 28, 2020; Accepted July 19, 2020; Epub October 15, 2020; Published October 30, 2020

**Abstract:** Objective: Our study aimed to investigate the mechanism by which miR-217 regulates pancreatic β cell functions by targeting the KRAS gene in type 2 diabetic mice. Methods: We used a dual luciferase reporter assay to confirm that KRAS is a target to which miR-217 binds. HE staining was used to observe the morphology of the islets. The fasting blood glucose levels (FBG), fasting insulin levels (FINS), and the homeostatic model assessment for insulin resistance (HOMA-IR) levels were measured. The cell proliferation and apoptosis were compared. qRT-PCR and Western blot were applied to measure the mRNA and protein expressions. Results: The fasting blood glucose levels (FBG), fasting insulin levels (FINS), and homeostatic model assessment for insulin resistance (HOMA-IR) levels were significantly increased in the type 2 diabetic model mice compared with the levels in the control mice. However, if the diabetic model mice were transfected with a miR-217 inhibitor and/or the KRAS overexpression plasmid pcDNA3.0-KRAS, the increases in the FBG, FINS, and HOMA-IR levels could be reversed. Regarding the in vitro transfections, the β cells harvested from the type 2 diabetic model mice exhibited decreased cell viability and increased apoptosis. In addition, the expression of miR-217 was upregulated, and KRAS was downregulated. Transfection with either the miR-217 inhibitor or with pcDNA3.0-KRAS increased β cell viability and decreased apoptosis. Co-transfection with the miR-217 inhibitor and pcDNA3.0-KRAS further enhanced these effects on the β cells. Conclusion: miR-217 silencing promotes pancreatic β cell proliferation and inhibits β cell apoptosis by upregulating KRAS expression, and this outcome is conducive to the alleviation of insulin resistance in type 2 diabetic model mice.

**Keywords:** miR-217, KRAS, type 2 diabetic model mice, pancreatic β cell, proliferation

## Introduction

Diabetes is regarded as one of the world's major health problems. Type 2 diabetes mellitus (T2DM), also known as non-insulin-dependent diabetes, is characterized by hyperglycemia due to insulin resistance and β cell dysfunction, accounting for at least 90% of the total number of people with diabetes [1-3]. At present, the number of Chinese patients with T2DM ranks first in the world and is increasing annually with the development of China. Because the high prevalence of T2DM seriously threatens the health of residents in China, research on the pathogenesis of T2DM is urgently needed to provide a theoretical basis for its clinical treatment.

MicroRNAs (miRNAs) are non-coding RNAs of approximately 22 nt in length and found in a wide variety of organisms, from viruses to humans. As a member of the miRNA family, miR-217 is upregulated in patients with diabetic nephropathy (DN) and in rat glomerular mesangial cells cultured in high glucose medium [7, 8]. The expression of miR-217 is also positively correlated with the homeostatic model assessment for the insulin resistance (HOMA-IR) score and the total cholesterol levels [9-12]. A number of recent studies have confirmed that miR-217 may be involved in the development of proteinuria in patients with T2DM, and miR-217 may participate in the development of DN by promoting chronic inflammation, renal fibrosis and angiogenesis [13-16]. Our bioinformatics analysis revealed a binding site that facilitates interaction between miR-217 and KRAS. Additionally, we found in the literature that KRAS mutations may lead to the development of

renovascular hypertension, congenital lipomatosis and diabetes [17-20]. Therefore, we speculated that miR-217 may regulate insulin resistance in mice with T2DM by targeting and regulating the KRAS gene.

In this study, a mouse model of T2DM was established, and we performed in vitro and in vivo transfections using the miR-217 inhibitor and the KRAS overexpression plasmid. Our study aimed to explore the regulation mechanism of miR-217 and KRAS on the pancreatic β-cell function and insulin resistance.

## Materials and methods

### *Dual luciferase reporter assay*

A bioinformatics analysis (www.targetscan.com) showed that miR-217 has a putative binding site for the KRAS gene. A dual luciferase reporter assay was performed to verify the targeting relationship between miR-217 and KRAS. The 3'UTR of the KRAS gene was amplified and inserted downstream of the firefly luciferase gene in the pmirGLO vector (Promega, USA), and the construct was named Wt-KRAS. The 3'UTR of the KRAS gene with a mutated binding site was inserted downstream of the firefly luciferase gene in the pmirGLO vector, and the construct was named Mut-KRAS. Then, an miR-217 inhibitor or an miR-217 inhibitor negative control (NC) was co-transfected with the dual luciferase reporter plasmid into normal β cells according to the instructions provided by Promega.

### *Animals*

A total of 85 specific pathogen-free, 8-week-old male C57BL/6J mice weighing 20-25 g were purchased from Beijing Vital River Laboratory Animals Inc. All the animals were raised in a pathogen-free environment at 25±1°C and 40-70% humidity with a 12-hour light/12-hour dark cycle. All the animals had free access to food and drink. The animal work was performed at the Wuhan Institute of Physics and Mathematics, and this study was approved by the Animal Care and Use Committee of the Wuhan Institute of Physics and Mathematics (no. 20180812).

### *Animal modeling and grouping*

Upon arrival, 15 mice were randomly selected as the normal group and fed a normal diet. The other 70 mice were fed a high-sugar and high-fat diet (5% lard and 5% sugar, Beijing Bo'ao Harbor Business Center) for one month, followed by daily intraperitoneal injections with 40 mg/kg streptozotocin (STZ, Sigma) for 5 days. The normal group received vehicle (50 mM sodium citrate, pH 4.5) injections for 5 days. A glucometer (Roche, Germany) was used to measure the tail blood glucose levels at 8 a.m. after fasting for 12 hours. The generation of the model was considered successful if the fasting blood glucose (FBG) levels were higher than 11.1 mmol/L for 3 consecutive days.

Of the mice in which the disease model was successfully established, 50 mice were randomly selected and divided into 5 groups with 10 mice in each group: the model group (type 2 diabetic model mice), the NC group (type 2 diabetic model mice injected with the empty transfection agent through the caudal vein), the miR-217 inhibitor group (type 2 diabetic model mice transfected with the miR-217 inhibitor through the caudal vein), the oe-KRAS group (type 2 diabetic model mice transfected with pcDNA3.0-KRAS through the caudal vein), and the miR-217 inhibitor + oe-KRAS group (type 2 diabetic model mice co-transfected with the miR-217 inhibitor and pcDNA3.0-KRAS through the caudal vein). All the mice received caudal vein injections once a week for 4 consecutive weeks. The miR-217 inhibitor and pcDNA3.0-KRAS were purchased from Shanghai GenePharma Pharmaceutical Technology Co., Ltd., China.

### *Determination of the FBG levels*

After fasting for 12 h, the mice were anesthetized with 3% sodium pentobarbital at a dose of 30 mg/kg (Sigma, USA), and a 200 μL blood sample was withdrawn from the retro-orbital sinus. The blood samples were allowed to stand at room temperature for 2 h and then centrifuged at 3,000 r/min for 20 min to separate the serum. The serum was collected into a 1 mL EP tube and stored at -80°C for later use. The FBG levels were measured using a glucose oxidase assay kit (Beijing Biosino Biotechnology Co., Ltd.). The absorbance value of each sample at a wavelength of 505 nm, which is proportional to the glucose level, was measured using a microplate reader (Hitachi, Japan).

*Determination of the fasting insulin (FINS) levels*

The FINS was measured using an enzyme-linked immunosorbent assay (ELISA) kit (Solarbio, China) in accordance with the manufacturer's instructions. The standard reference and samples were loaded in the microplate, and HRP-labeled insulin antibody was added to form a complex with the sample. After applying the chromogenic substrate TMB, the absorbance value was measured at a wavelength of 450 nm to calculate the insulin concentration of each sample based on the standard curve.

*Hematoxylin-eosin (HE) staining*

After the blood collection, the anesthetized mice died of excessive blood loss with their heartbeats stopping and pupils diffusing. The pancreas was promptly harvested and immersed in 10% formaldehyde. Paraffin sections were made and dewaxed with xylene. The sections were dehydrated using a gradient of ethanol and then rinsed with distilled water for 2 min. Hematoxylin and eosin was used to stain the sections for 5 min. The sections were then deparaffinized and sealed with resinene. An optical microscope (Bingyu Optical Instrument Co., Ltd., China) was used to observe the morphological changes of the islet cells.

*HOMA-IR*

HOMA-IR was calculated using the following formula: HOMA-IR = FBG * FINS/22.5. HOMA-IR is an indicator of insulin resistance, and a higher value represents more severe insulin resistance.

*Isolation of pancreatic β cells*

Pancreatic tissue was harvested from the mice in the normal and model groups. The specimens were rinsed twice with PBS to remove the excess fat and lymphatic nodes and were cut using microsurgery scissors. The pancreatic β cells were isolated using cold trypsin-EDTA digestion. The cells were then seeded in culture flasks with DMEM/F12 medium containing 20% fetal bovine serum (Jingke Chemical Technology Co., Ltd., China). The cells were cultured in an incubator with 5% $CO_2$ at 37°C. When the cells reached 80-90% confluence, 2 mL of 0.25% trypsin (GIBCO, USA) was added for 3 min for digestion, and then the medium was replaced by DMEM/F12 containing 10% serum. The cell suspension was collected by repeated pipetting and centrifuged at 1,000 r/min for 6-8 min at 4°C. The cells were then subcultured in a complete medium (Innovare Biomedical, China) at a ratio of 1:3.

*Cell grouping and transfection*

Pancreatic β cells from the normal and the model groups were seeded into 6-well plates at a density of $1*10^5$ cells/well, with 3 replicate wells for each group. The β cells were divided into 6 groups: the normal group (β cells from the normal group), the model group (β cells from the model group), the NC group (β cells from the model group transfected with an empty transfection agent), the miR-217 inhibitor group (β cells from the model group transfected with the miR-217 inhibitor), the oe-KRAS group (β cells from the model group transfected with pcDNA3.0-KRAS), and the miR-217 inhibitor + oe-KRAS group (β cells from the model group co-transfected with the miR-217 inhibitor and pcDNA3.0-KRAS). The miR-217 inhibitor and pcDNA3.0-KRAS (50 nmol/L, Vigenebio, USA) were centrifuged and mixed with 170 μL PBS. The mixture was allowed to sit for 5 min before 30 μL Lipofectamine 2000 (Thermo Fisher, USA) was added. The transfection was performed in strict accordance with the manufacturer's instructions. At 6 h after the transfection, the medium was replaced with DMEM/F12 containing 10% fetal bovine serum.

*Determination of the cell viability using an MTT assay*

At 48 h after the transfection, the pancreatic β cells were digested and seeded into 96-well plates at a density of $3\text{-}6*10^3$ cells/well in a volume of 100 μL/well. Each group included 6 replicate wells. At 24 h, 48 h, and 72 h after the transfection, 20 μL of MTT solution (GIBCO, USA) at a concentration of 5 mg/mL was added to each well, and the incubation was continued for another 4 h. Then, 100 μL DMSO was added to each well and gently mixed for 10 min. A microplate reader (Beijing Noah Instrument Co., Ltd., China) was used to measure the absorbance value (the OD value) of each well at a wavelength of 490 nm. The assay was performed 3 times, and the cell viability curve was plotted with each time point as the abscissa and the OD value as the ordinate.

**Table 1.** The qRT-PCR primer sequence

| Gene | Sequence |
|---|---|
| miR-217 | F: 5'-ATGTTGCGGACTTGCTATCTGT-3' |
| | R: 5'-AGTAGAATGTGTGGGTGATCCT-3' |
| KRAS | F: 5'-CTCTAGTTCTGGATACCTAG-3' |
| | R: 5'-TACTGTGTGCCAGTCACAGC-3' |
| U6 | F: 5'-CAATATGCCCTCGACGGGTA-3' |
| | R: 5'-CGCACCACGGACACATGACT-3' |
| GAPDH | F: 5'-GGGCTGCTTTTAACTCTGGT-3' |
| | R: 5'-GCAGGTTTTTCTAGACGG-3' |

*Determination of the cell cycle and apoptosis using flow cytometry*

The pancreatic β cells were collected 48 h after transfection. The cells were washed 3 times with PBS and centrifuged at 3,000 r/min for 20 min. The supernatant was discarded, and the cell density was adjusted to $1*10^6$/mL. The cells were fixed by adding 1 mL cold 75% ethanol at 4°C for 1 h. Then the cells were washed twice with PBS before adding 100 μL RNase A (Thermo Fisher, USA). A volume of 400 μL PI (Sigma, USA) was added to stain the cells, and then, the cell cycle stages were assessed using a flow cytometer (Beckman Coulter, USA) to measure the red fluorescence at a wavelength of 488 nm.

At 48 h after the transfection, the pancreatic β cells were digested using trypsin (Thermo Fisher, USA) without EDTA and then collected in a sample tube. The sample tube was centrifuged at 3,000 r/min for 30 min, and the supernatant was discarded. The cells were washed 3 times with cold PBS before adding 100 μL Annexin-V-FITC/PI staining solution. The staining solution was made by mixing HEPES buffer, Annexin-V-FITCm and PI at a ratio of 50:1:2. The mixture was incubated at room temperature for 15 min. The cellular apoptosis was assessed by measuring the FITC and PI fluorescence at an excitation wavelength of 488 nm and emission wavelengths of 525 and 575 nm, respectively. The experiment was repeated three times.

*Quantitative real-time PCR (qRT-PCR)*

At 48 h after the transfection, the pancreatic β cells were harvested, and the total RNA was extracted using the TRIzol reagent (Invitrogen, USA). The RNA was reverse transcribed into cDNA using a Reverse Transcription Kit (Merck, USA). The PCR mixture was prepared using the SYBR® Premix Ex Taq™ II Kit (Xingzhi Biotechnology Co., Ltd., China). The total reaction volume was 50 μL, and it contained the following: 25 μL SYBR® Premix Ex Taq™ II (2×), 2 μL upstream primer, 2 μL downstream primer, lμL ROX Reference Dye (50×), 4 μL DNA template, and 16 μL $ddH_2O$. qRT-PCR was performed using an ABI 7900HT system (ABI, USA). The reaction conditions were as follows: predenaturation at 95°C for 30 s, denaturation at 95°C for 5 s, annealing at 58°C for 30 s, and extension at 72°C for 15 s. The cycle was repeated 40 times. The relative expression level of each gene was calculated using the $2^{-\Delta\Delta Ct}$ method with GAPDH as the internal reference for KRAS and U6 as the internal reference for miR-217: $\Delta Ct = CT_{(gene\ of\ interest)} - CT_{(internal\ reference)}$. The reaction was repeated 3 times. The primers are listed in **Table 1**.

*Western blot*

The pancreatic β cells were digested and harvested at 48 h after transfection, and the total protein was extracted using a RIPA buffer containing PMSF (Solarbio Life Science Co., Ltd., China). The protein concentration was measured using a BCA kit (Thermo Fisher, USA) and adjusted with deionized water. The samples were mixed with a loading buffer and boiled for 10 min. A total of 20 μg protein per sample was added to each lane of a 12% SDS-PAGE gel (Biolab Technology Co., Ltd., China). Electrophoresis was carried out at 80 V for 2 h. The protein was transferred to a PVDF membrane (Millipore, USA) at a voltage of 110 V for 2 h. The membrane was then blocked with 5% skim milk at 4°C for 2 h. After discarding the blocking solution, the membrane was washed with TBST (Solarbio, China) and incubated with the following primary antibodies overnight at 4°C: rabbit anti-human KRAS (1:500, Abcam, UK) and GAPDH (1:2,000, Abcam, UK). Then, the membrane was incubated with HRP-labeled goat anti-rabbit IgG antibodies (1:5,000, Beijing Zhongshan Biotechnology Co., Ltd., China) for 2 h at room temperature. The membrane was washed 3 times with TBST before a DAB horseradish peroxidase color development solution was applied. The membrane was exposed and photographed with a Bio-Rad image analysis system (BIO-RAD, USA). ImageJ software was used to calculate the relative expres-

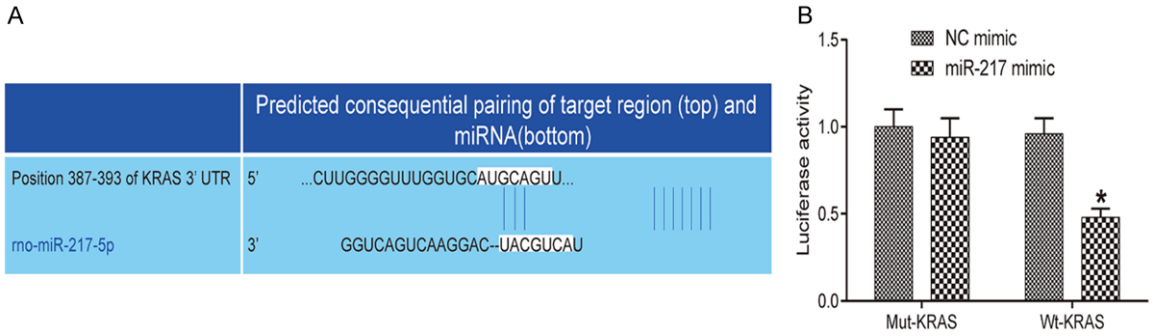


**Figure 1.** The KRAS gene is a target to which miR-217 binds. A: The binding sequence of miR-217 and KRAS 3'-UTR; B: Relative luciferase activity. *P<0.05, compared with the miR-217 mimic negative control. NC: negative control.

sion by comparing the gray value of the protein of interest with the gray value of GAPDH. The experiment was repeated 3 times.

*Statistical analysis*

All the data were analyzed using SPSS 21.0 software. The quantitative data are expressed as the mean ± standard deviation ($\bar{x}$ ± sd). The comparisons between multiple groups were analyzed using one-way ANOVA, followed by Bonferroni's post-hoc comparisons. A *P* value less than 0.05 was considered statistically significant.

## Results

*miR-217 can target the KRAS gene*

The bioinformatics analysis using online software TargetScan (www.targetscan.com) indicated that the 3'UTR of KRAS the gene has a putative binding site for miR-217 (**Figure 1A**). A dual luciferase reporter assay showed that β cells co-transfected with the miR-217 mimic and Wt-KRAS had significantly lower luciferase activity than the cells transfected with the miR-217 mimic NC and Mut-KRAS (all P<0.05, **Figure 1B**). The results indicated that KRAS is a target to which miR-217 binds.

*HE staining*

HE staining was performed to observe the pancreatic islet morphology in each group (**Figure 2**). The islet cells in the normal group were arranged neatly and exhibited regular cell sizes, and they had mostly round nuclei and clear chromatin. In contrast, the islets in the model group and the NC group were decreased in number and were atrophic and arranged irregularly with vacuolar degeneration. Pyknosis and lysis were observed in the islet tissues, and the presence of lymphocytes and monocytes indicated tissue inflammation. In the miR-217 inhibitor group, the oe-KRAS group, and the miR-217 inhibitor + oe-KRAS group, the islets appeared relatively normal with minor bleeding and vacuolar degeneration, and the number of cells was mildly decreased.

*FBG, FINS, and HOMA-IR levels*

The FBG (**Figure 3**) and FINS levels (**Figure 4**) in each group were measured, and the HOMA-IR values (**Figure 5**) were calculated. Compared with the normal group, the FBG, FINS, and HOMA-IR levels in the other groups were increased (all P<0.05). No differences were observed between the NC group and model group in the levels of these markers (all P> 0.05). Compared with the model group, the FBG, FINS, and HOMA-IR levels were decreased in the miR-217 inhibitor group, the oe-KRAS group, and the miR-217 inhibitor + oe-KRAS group (all P<0.05). The miR-217 inhibitor + oe-KRAS group showed more decreased FBG, FINS, and HOMA-IR levels than both the miR-217 inhibitor group and the oe-KRAS group (all P<0.05). Silencing miR-217 or overexpressing KRAS reduced the FBG, FINS, and HOMA-IR levels in the type 2 diabetic mice.

*MTT assay*

The comparison of the β cell viability in each group is shown in **Figure 6**. Compared with the normal group, the β cell viability in the other groups was decreased at 48 h and 72 h (all P<0.05). Compared with the model group, the

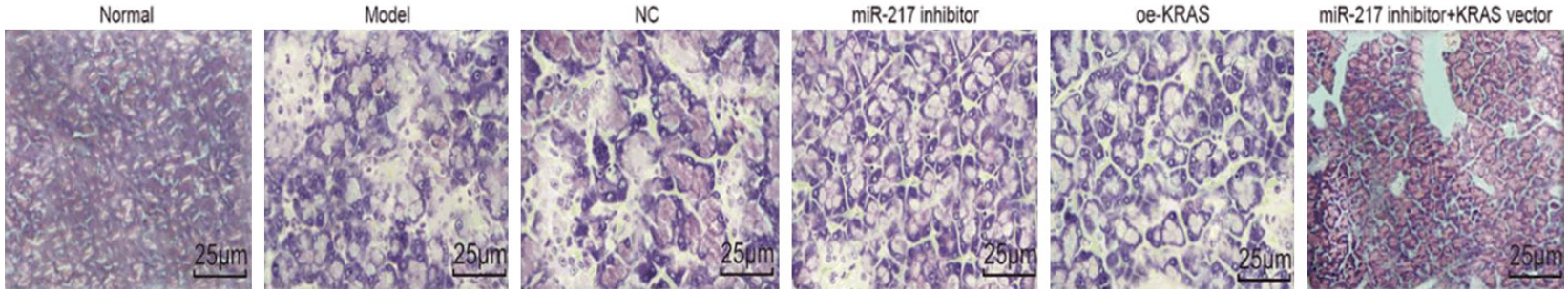


**Figure 2.** HE staining of the pancreatic tissue (200×). HE: hematoxylin-eosin; NC: negative control.

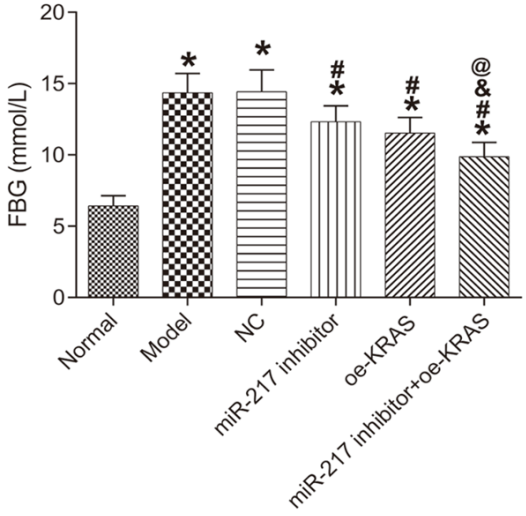


**Figure 3.** Comparison of the fasting blood glucose levels. FBG: Fasting blood glucose; NC: negative control. *P<0.05, compared with the normal group; #P<0.05, compared with the model group; &P<0.05, compared with the miR-217 inhibitor group; @P<0.05, compared with the oe-KRAS group.

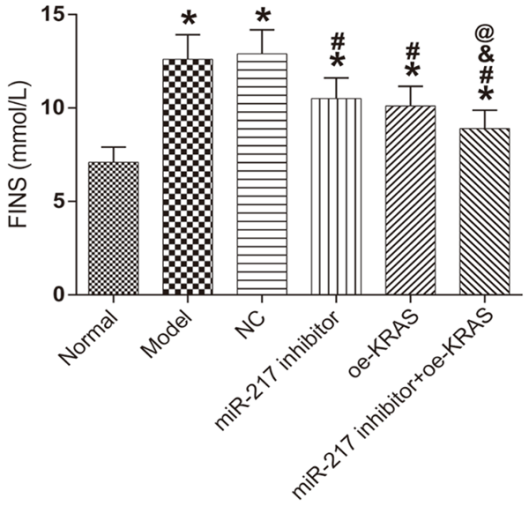


**Figure 4.** Comparison of the fasting insulin levels. FINS: Fasting insulin; NC: negative control. *P<0.05, compared with the normal group; #P<0.05, compared with the model group; &P<0.05, compared with the miR-217 inhibitor group; @P<0.05, compared with the oe-KRAS group.

β cell viability in the miR-217 inhibitor group, the oe-KRAS group, and the miR-217 inhibitor + oe-KRAS group were increased (all P<0.05). There were no differences between the model group and the NC group at all time points (all P>0.05). The β cell viability in the miR-217 inhibitor + oe-KRAS group was higher than it was in the miR-217 inhibitor group and the oe-KRAS group (all P<0.05). Silencing the miR-217 or overexpressing the KRAS significantly increased β cell viability in the type 2 diabetic model mice.

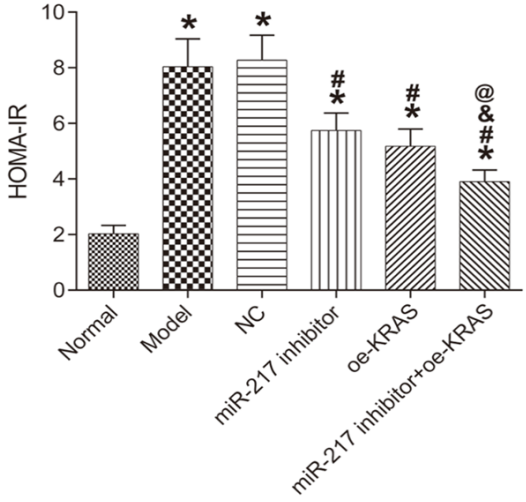


**Figure 5.** Comparison of the HOMA-IR. HOMA-IR: Homeostatic Model Assessment for Insulin Resistance; NC: negative control. *P<0.05, compared with the normal group; #P<0.05, compared with the model group; &P<0.05, compared with the miR-217 inhibitor group; @P<0.05, compared with the oe-KRAS group.

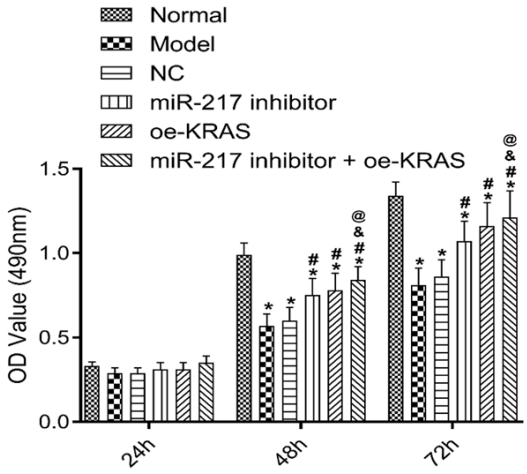


**Figure 6.** Comparison of the β cell viability. OD: Optical density; NC: negative control. *P<0.05, compared with the normal group; #P<0.05, compared with the model group; &P<0.05, compared with the miR-217 inhibitor group; @P<0.05, compared with the oe-KRAS group.

*β cell cycle*

Flow cytometry was used to determine the cell cycle in each group (**Figure 7**). Compared with the normal group, the proportions of β cells in

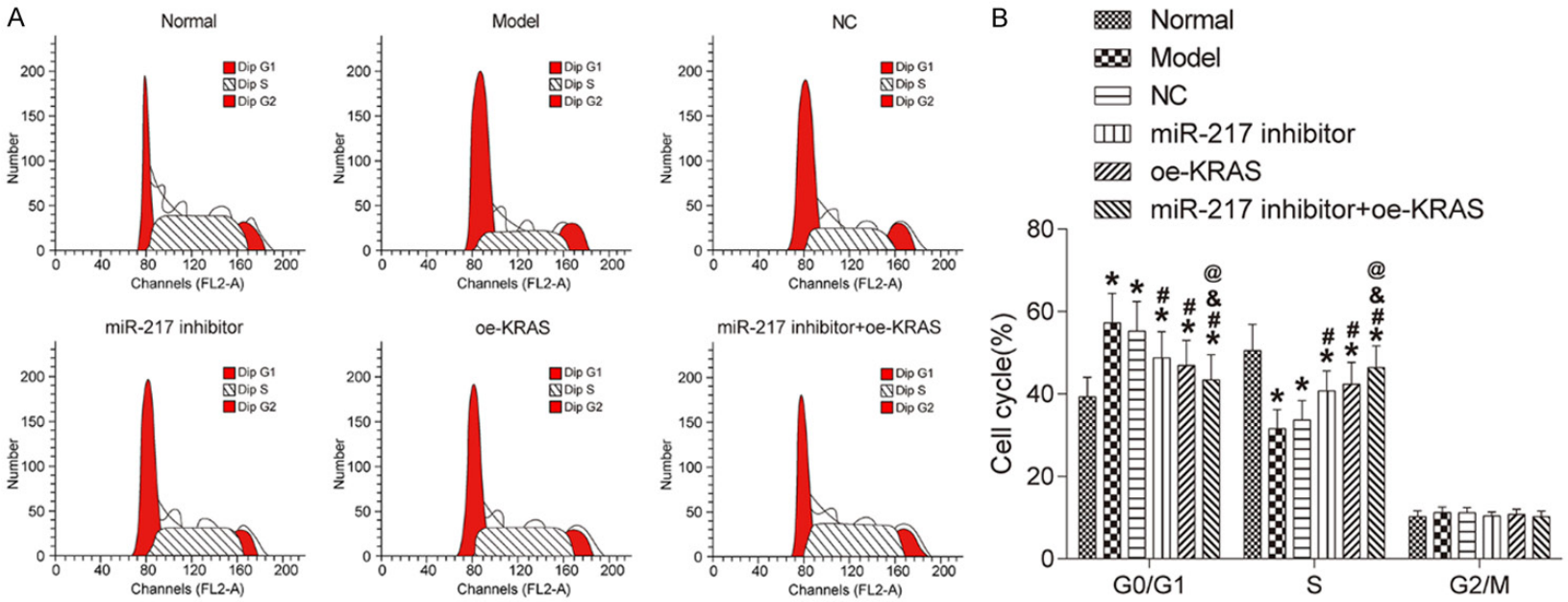


**Figure 7.** Comparison of the β cell cycles using flow cytometry. A: The growth cycles of pancreatic β cells in each group; B: Statistical diagram of the pancreatic β cell growth cycle in each group. NC: negative control. *P<0.05, compared with the normal group; #P<0.05, compared with the model group; &P<0.05, compared with the miR-217 inhibitor group; @P<0.05, compared with the oe-KRAS group.

the G1 phase were increased in the other groups, but the proportions of β cells in the S phase were decreased (all P<0.05). Compared with the model group, the proportions of β cells in the G1 phase were decreased in the miR-217 inhibitor group, the oe-KRAS group, and the miR-217 inhibitor + oe-KRAS group; however, the proportions of the β cells in the S phase were increased (all P<0.05). No differences were observed between the model group and the NC group in the distribution of the cell cycles (all P>0.05). The miR-217 inhibitor + oe-KRAS group had a lower proportion of β cells in the G1 phase and a higher proportion of β cells in the S phase compared with the miR-217 inhibitor group and the oe-KRAS group (all P<0.05).

*β cell apoptosis*

The cellular apoptosis was measured using flow cytometry (**Figure 8**). Compared with the normal group, the β cell apoptosis rates in the other groups were increased (all P<0.05). Compared with the model group, the β cell apoptosis rates in the miR-217 inhibitor group, the oe-KRAS group, and the miR-217 inhibitor + oe-KRAS group were decreased (all P<0.05). There were no differences between the model group and the NC group (P>0.05). The β cell apoptosis rate in the miR-217 inhibitor + oe-KRAS group was lower than it was in the miR-217 inhibitor group and the oe-KRAS group (all P<0.05). Silencing miR-217 or overexpressing KRAS significantly inhibited β cell apoptosis in type 2 diabetic model mice.

*miR-217 and KRAS expressions in pancreatic β cells*

The qRT-PCR and Western blot results are shown in **Figure 9**. Compared with the normal group, the model group had an increased expression level of miR-217 and decreased mRNA and protein expression levels of KRAS (all P<0.05). Compared with the model group, the expression level of miR-217 was decreased in the miR-217 inhibitor group and in the miR-217 inhibitor + oe-KRAS group, and the mRNA and protein expression levels of KRAS were increased in the miR-217 inhibitor group, the oe-KRAS group, and the miR-217 inhibitor + oe-KRAS group (all P<0.05). There were no differences between the model group and the NC group in terms of their miR-217 and KRAS expressions (all P>0.05).

## Discussion

microRNAs, widely existing in mammals, have a very important regulatory role in biological functions. miR-217, a member of the miRNA family, has a high expression level in diabetics and has a significant regulation effect on insulin resistance and blood glucose levels [21-24]. Li et al. found that in diabetic nephropathy, the upregulation of miR-217 can lead to an increase in oxidative stress [25]. In addition, Wang et al. suggested that miR-217 can be used as a potential biomarker for acute pancreatic exocrine toxicity in rats, and the expression of miR-217 was significantly upregulated after pancreatic injury [26]. In this study, we established a mouse model of T2DM and transfected the model mice with miR-217 inhibitors and KRAS overexpression plasmids. The results showed that the expression of miR-217 was significantly upregulated in the type 2 diabetic model mice compared to the normal mice. Compared with the model group, the FBG, FINS, and insulin resistance index HOMA-IR levels were significantly lower in the miR-217 inhibitor-transfected mice. In addition, we isolated pancreatic β cells from the normal and model mice and transfected the pancreatic β cells from the model mice with a miR-217 inhibitor. We found that the miR-217 inhibitor group showed significantly increased β cell viability and decreased cellular apoptosis compared to the other groups. The results indicated that miR-217 is upregulated in type 2 diabetic mice. The inhibition of miR-217 could lower the FBG levels and alleviate insulin resistance; moreover, pancreatic β cell functions were improved by promoting β cell viability and inhibiting cell apoptosis.

At present, several studies have shown that the KRAS mutation can lead to the occurrence of renal vascular hypertension, congenital lipomatosis, and diabetes [27-29]. The results of this study showed that the FBG, FINS and HOMA-IR levels were significantly decreased in the miR-217 inhibitor and oe-KRAS groups compared to the model group. In addition, the β cell viability was increased, and the cellular apoptosis was decreased in the two groups. These changes were even more pronounced in the group that was co-transfected with the miR-217 inhibitor

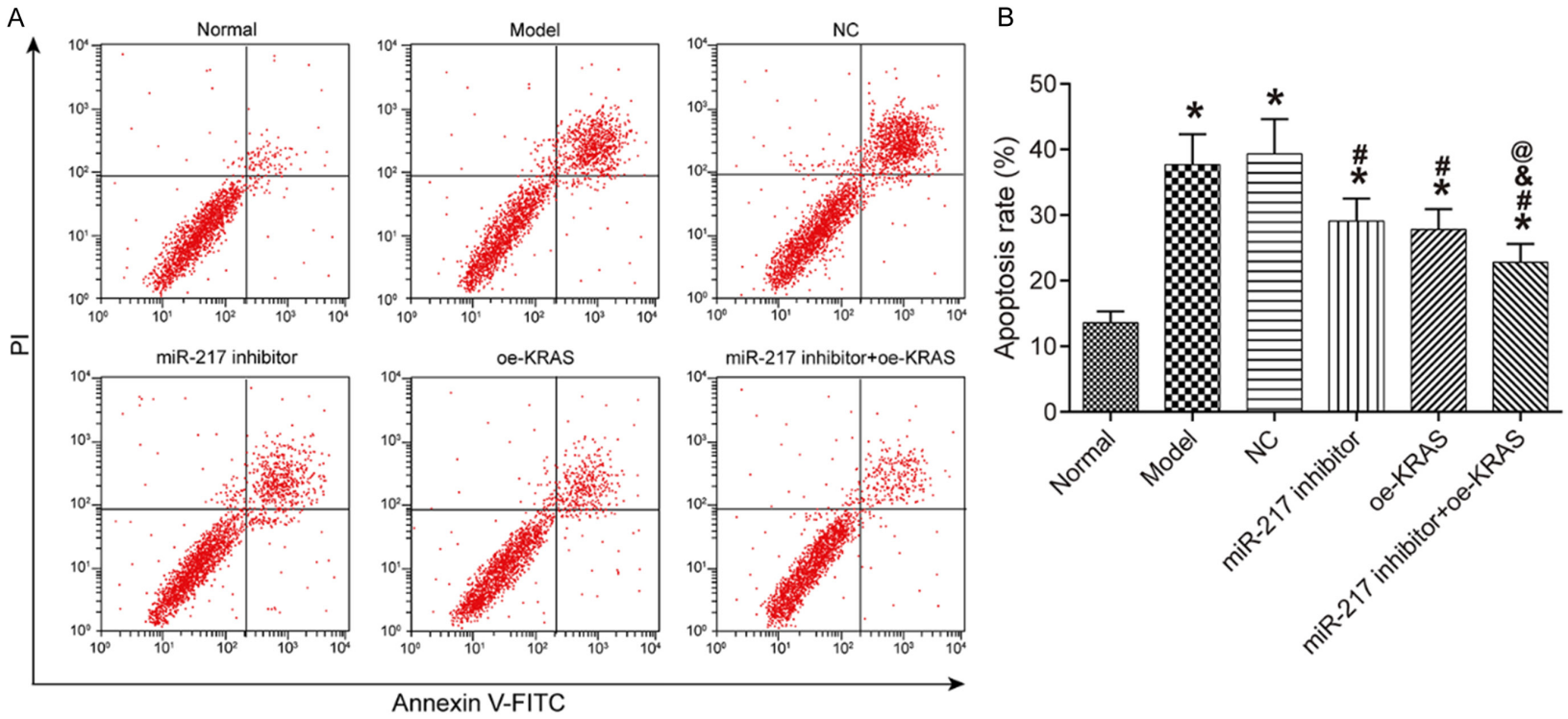


**Figure 8.** Comparison of the β cell apoptosis using flow cytometry. A: The apoptosis of pancreatic β cells in each group; B: Statistical diagram of the pancreatic β cell apoptosis in each group. NC: negative control. *P<0.05, compared with the normal group; #P<0.05, compared with the model group; &P<0.05, compared with the miR-217 inhibitor group; @P<0.05, compared with the oe-KRAS group.

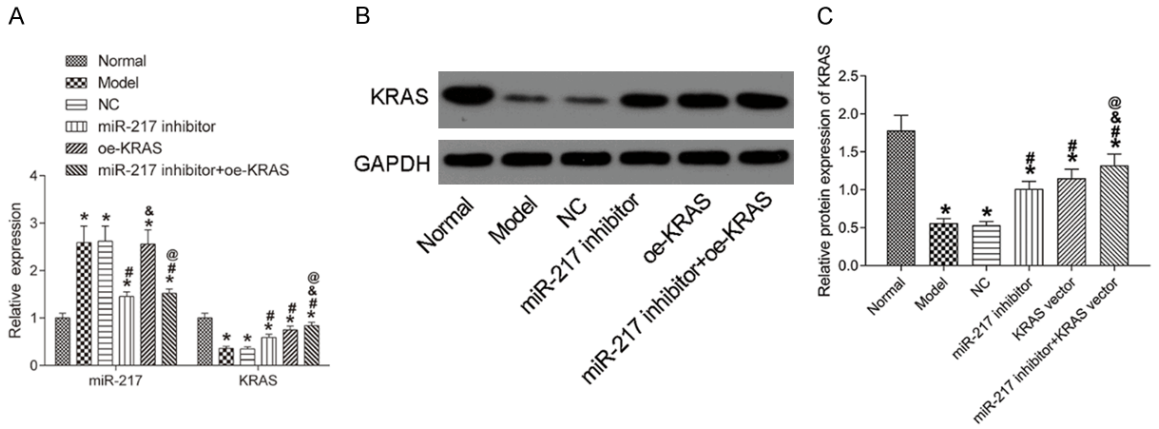


**Figure 9.** Comparison of the mRNA and protein expression levels of the β cell related genes using qRT-PCR and Western blot. A: The expression levels of miR-217 and KRAS mRNA in each group; B and C: The expression levels of the KRAS protein in each group. NC: negative control. *P<0.05, compared with the normal group; #P<0.05, compared with the model group; &P<0.05, compared with the miR-217 inhibitor group; @P<0.05, compared with the oe-KRAS group.

and oe-KRAS. Together, these results show that after silencing miR-217 in type 2 diabetic mice, the expression of KRAS is significantly increased due to decreased inhibition; therefore, the mice have lower FBG levels, decreased insulin resistance, and better β cell functions.

However, there are still some limitations to this study. First, due to some technical limitations, we did not quantify the purity of the pancreatic β cells and only examined the purity through observation under a microscope. It is unclear whether the presence of small number of other cells, such as duct cells, acinar cells, and pancreatic α-cells, may influence our study results. Second, in light of the fact that the β cell functions in the miR-217 inhibitor + oe-KRAS group were significantly better than they were in the miR-217 inhibitor group or oe-KRAS group, we speculate that miR-217 may regulate β cell functions through other signaling pathways. The specific link between miR-217 and KRAS and the regulatory network of miR-217 have not yet been fully defined. By using RNA-Seq, we may find more clues to make the mechanism clear. Moreover, whether miR-217 and KRAS can be used as therapeutic targets requires further clinical experiments.

In conclusion, we confirmed that miR-217 can downregulate the expression of KRAS, leading to impaired insulin sensitivity and pancreatic β cell functions in type 2 diabetic mice.

## Acknowledgements

This work was supported by the Joint Project Yunnan Science and Technology Department-Kunming Medical University (2019FE001 (-112)).

## Disclosure of conflict of interest

None.

**Address correspondence to:** Ling Li, Biomedical Engineering Research Center, Kunming Medical University, No. 1168 Chunrong West Road, Yuhua Street, Chenggong District, Kunming 650500, Yunnan Province, China. Tel: +86-13888657164; E-mail: lilingky26@163.com; Xi'nan Wu, The School of Public Health, Kunming Medical University, No. 1168 Chunrong West Road, Yuhua Street, Chenggong District, Kunming 650500, Yunnan Province, China. Tel: +86-13888984762; E-mail: wuxinany-7n2@163.com

## References

[1] Shi TS, Lu K, Shen SY, Tang QL, Zhang KJ, Zhu XB, Shi Y, Liu XL, Teng HJ, Li CJ, Xue B and Jiang Q. Fenofibrate decreases the bone quality by down regulating Runx2 in high-fat-diet induced type 2 diabetes mellitus mouse model. Lipids Health Dis 2017; 16: 201.

[2] Xiong MR, Huang Y, Liu YJ, Huang M, Song GJ, Ming Q, Ma XH, Yang J, Deng SH, Wen YZ, Shen JH, Liu QH, Zhao P and Yang XZ. Antidiabetic activity of ergosterol from pleurotus ostreatus

in KK-A(y) mice with spontaneous type 2 diabetes mellitus. Mol Nutr Food Res 2018; 62.
[3] Xu FF, Wang N, Li GQ, Guo WF, Yang CF and Liu DH. Establishment and assessment of mice models of type 2 diabetes mellitus. Acta Academ Med Sinicae 2017; 39: 324-329.
[4] Cha S, Lee SH, Kang SH, Hasan MN, Kim YJ, Cho S and Lee YK. Antibody-mediated oral delivery of therapeutic DNA for type 2 diabetes mellitus. Biomater Res 2018; 22: 19.
[5] Chattopadhyay T, Singh RR, Gupta S and Surolia A. Bone morphogenetic protein-7 (BMP-7) augments insulin sensitivity in mice with type II diabetes mellitus by potentiating PI3K/AKT pathway. Biofactors 2017; 43: 195-209.
[6] Erickson RL, Browne CA and Lucki I. Hair corticosterone measurement in mouse models of type 1 and type 2 diabetes mellitus. Physiol Behav 2017; 178: 166-171.
[7] Bai M, Zhang MZ, Long F, Yu NZ, Zeng A and Wang XJ. MiR-217 promotes cutaneous squamous cell carcinoma progression by targeting PTRF. Am J Transl Res 2017; 9: 647-655.
[8] Zheng J, Liu XB, Xue YX, Gong W, Ma J, Xi Z, Que ZY and Liu YH. TTBK2 circular RNA promotes glioma malignancy by regulating miR-217/HNF1β/Derlin-1 pathway. J Hematol Oncol 2017; 10: 52.
[9] Bao B, Wang ZW, Li YW, Kong DJ, Ali S, Banerjee S, Ahmad A and Sarkar FH. The complexities of obesity and diabetes with the development and progression of pancreatic cancer. Biochim Biophys Acta 2011; 1815: 135-146.
[10] Li J, Liu B, Xue H, Zhou QQ and Peng L. miR-217 is a useful diagnostic biomarker and regulates human podocyte cells apoptosis via targeting TNFSF11 in membranous nephropathy. Biomed Res Int 2017; 2017: 2168767.
[11] Shao Y, Lv C, Wu C, Zhou YH and Wang QY. Mir-217 promotes inflammation and fibrosis in high glucose cultured rat glomerular mesangial cells via Sirt1/HIF-1α signaling pathway. Diabetes Metab Res Rev 2016; 32: 534-543.
[12] Shao Y, Ren HW, Lv C, Ma XY, Wu C and Wang QY. Changes of serum Mir-217 and the correlation with the severity in type 2 diabetes patients with different stages of diabetic kidney disease. Endocrine 2017; 55: 130-138.
[13] Hillman Y, Mazkereth N, Farberov L, Shomron N and Fishelson Z. Regulation of complement-dependent cytotoxicity by microRNAs miR-200b, miR-200c, and miR-217. J Immunol 2016; 196: 5156-5165.
[14] Li JY, Li DM and Zhang WY. Tumor suppressor role of miR-217 in human epithelial ovarian cancer by targeting IGF1R. Oncol Rep 2016; 35: 1671-1679.
[15] Ono K, Kuwabara Y and Han J. MicroRNAs and cardiovascular diseases. FEBS J 2011; 278: 1619-1633.
[16] Wang T, Mu CZ, Wang XM, Tian H and Chen XS. Role of miR-217 in target regulation of differentiated NeuroD1 gene expression induced by insulin-secreting cells. Acad J Chin PLA Med 2013; 34: 1063-1066.
[17] Gomes CC, de Sousa SF, de Menezes GH, Duarte AP, Pereira Tdos S, Moreira RG, de Castro WH, Villacis RA, Rogatto SR, Diniz MG and Gomez RS. Recurrent KRAS G12V pathogenic mutation in adenomatoid odontogenic tumours. Oral Oncol 2016; 56: e3-5.
[18] Groesser L, Herschberger E, Ruetten A, Ruivenkamp C, Lopriore E, Zutt M, Langmann T, Singer S, Klingseisen L, Schneider-Brachert W, Toll A, Real FX, Landthaler M and Hafner C. Postzygotic HRAS and KRAS mutations cause nevus sebaceous and Schimmelpenning syndrome. Nat Genet 2012; 44: 783-787.
[19] Holmes D. Diabetes: could broccoli have a role in combating type 2 diabetes mellitus? Nat Rev Endocrinol 2017; 13: 437.
[20] Kuroda Y, Ohashi I, Enomoto Y, Naruto T, Baba N, Tanaka Y, Aida N, Okamoto N, Niihori T, Aoki Y and Kurosawa K. A postzygotic NRAS mutation in a patient with Schimmelpenning syndrome. Am J Med Genet A 2015; 167A: 2223-2225.
[21] Flum M, Kleemann M, Schneider H, Weis B, Fischer S, Handrick R and Otte K. miR-217-5p induces apoptosis by directly targeting PRKCI, BAG3, ITGAV and MAPK1 in colorectal cancer cells. J Cell Commun Signal 2018; 12: 451-466.
[22] Khor ES and Wong PF. Endothelial replicative senescence delayed by the inhibition of MTORC1 signaling involves microRNA-107. Int J Biochem Cell Biol 2018; 101: 64-73.
[23] Sun J, Li ZP, Zhang RQ and Zhang HM. Repression of miR-217 protects against high glucose-induced podocyte injury and insulin resistance by restoring PTEN-mediated autophagy pathway. Biochem Biophys Res Commun 2017; 483: 318-324.
[24] Zhou WH, Song FF, Wu QJ, Liu R, Wang LL, Liu CC, Peng Y, Mao SQ, Feng J and Chen CS. miR-217 inhibits triple-negative breast cancer cell growth, migration, and invasion through targeting KLF5. PLoS One 2017; 12: e0176395.
[25] Li D, Lu ZY, Jia JY, Zheng ZF and Lin S. Changes in microRNAs associated with podocytic adhesion damage under mechanical stress. J Renin Angiotensin Aldosterone Syst 2013; 14: 97-102.
[26] Wang JY, Huang WH, Thibault S, Brown TP, Bobrowski W, Gukasyan HJ, Evering W, Hu WY,

John-Baptiste A and Vitsky A. Evaluation of miR-216a and miR-217 as potential biomarkers of acute exocrine pancreatic toxicity in rats. Toxicol Pathol 2017; 45: 321-334.

[27] Eibl G and Rozengurt E. KRAS, YAP, and obesity in pancreatic cancer: a signaling network with multiple loops. Semin Cancer Biol 2019; 54: 50-62.

[28] Eser S, Reiff N, Messer M, Seidler B, Gottschalk K, Dobler M, Hieber M, Arbeiter A, Klein S, Kong B, Michalski CW, Schlitter AM, Esposito I, Kind AJ, Rad L, Schnieke AE, Baccarini M, Alessi DR, Rad R, Schmid RM, Schneider G and Saur D. Selective requirement of PI3K/PDK1 signaling for Kras oncogene-driven pancreatic cell plasticity and cancer. Cancer Cell 2013; 23: 406-420.

[29] Fujimoto T and Shirasawa S. KRAS-induced actin-interacting protein: a potent target for obesity, diabetes and cancer. Anticancer Res 2011; 31: 2413-2417.